ORIGINAL PAPER

Divergent mineralization of hydrophilic and hydrophobic organic substrates and their priming effect in soils depending on their preferential utilization by bacteria and fungi

Shaohong Deng [1,2] · Xiaodong Zheng [1,3] · Xiangbi Chen [1,4] · Shengmeng Zheng [1,2] · Xunyang He [1] · Tida Ge [1] · Yakov Kuzyakov [5,6,7] · Jinshui Wu [1,2,4] · Yirong Su [1] · Yajun Hu [1,4]

Abstract

Hydrophilic and hydrophobic organic compounds extracted from ^{13}C-labelled maize residues were incubated with soils to evaluate their mineralization and priming effect (PE) caused by their utilization by microbial groups. Two soils with contrasting soil properties were collected from well-drained upland and water-logged paddy. Mineralization of the ^{13}C-labelled fractions and their PE were quantified by monitoring the CO_2 efflux and ^{13}C enrichment during a 40-day incubation. The composition of main microbial groups (bacteria and fungi) involved in the utilization of ^{13}C-labelled fractions was determined based on phospholipid fatty acids (PLFAs) analysis. At the initial stage (6–24 h), hydrophilic fraction had faster mineralization rate (3.6–70 times) and induced 1.5–10 times stronger PE (positive in upland soil and negative in paddy soil) than those of hydrophobic fraction. The ^{13}C-PLFAs data showed that the incorporation of hydrophilic fraction into bacteria was 11.4–16.4 times greater than that into fungi, whereas the hydrophobic fraction incorporated into fungi was 1.0–1.5 times larger than that into bacteria at day 2. This indicated greater contributions of r-strategists (fast-growing bacteria) for the uptake of hydrophilic fraction versus K-strategists (slow-growing fungi) for hydrophobic fraction. Compared with K-strategists, the r-strategists possessed a much faster metabolism and thus triggered stronger apparent PE by accelerating microbial biomass turnover, resulting in higher mineralization and stronger PE for the hydrophilic than hydrophobic fraction. The slower and less mineralization of both fractions in paddy than in upland soils is due to the suppression of microbial activity and substrate utilization under flooding. At the end of 40-day incubation, the cumulative mineralization of hydrophilic and hydrophobic fractions was similar. Consequently, microbial mechanisms underlying the utilization of organic compounds with contrasting solubility (hydrophilic or hydrophobic) are crucial for evaluating the stabilization and destabilization (e.g., priming) processes of soil organic matter.

Shaohong Deng and Xiaodong Zheng contributed equally to this work.

✉ Xiangbi Chen
xbchen@isa.ac.cn

✉ Yajun Hu
yjhu@isa.ac.cn

1 Key Laboratory of Agro-ecological Processes in Subtropical Region, Institute of Subtropical Agriculture, Chinese Academy of Sciences, Mapoling, Changsha City 410125, Hunan province, People's Republic of China

2 University of Chinese Academy of Sciences, Beijing 100039, People's Republic of China

3 Institute of Agricultural Resource and Environment, Guangdong Academy of Agricultural Science, Guangzhou 510640, Guangdong, People's Republic of China

4 Changsha Research Station for Agricultural and Environmental Monitoring, Institute of Subtropical Agriculture, Chinese Academy of Sciences, Mapoling, Changsha City 410125, Hunan province, People's Republic of China

5 Department of Agricultural Soil Science, Department of Soil Science of Temperate Ecosystems, University of Göttingen, 37077 Göttingen, Germany

6 Agro-Technological Institute, RUDN University, 117198 Moscow, Russia

7 Institute of Environmental Sciences, Kazan Federal University, 420049 Kazan, Russia

Introduction

As a byproduct of plant residue decomposition, dissolved organic matter (DOM) plays a crucial role in sustaining microbial functions in soil (Chen et al. 2018; Fan et al. 2020; Qiu et al. 2015). Microbial availability of DOM depends on its chemical recalcitrance, mineral association, and accessibility to decomposers and consequently determines its biological cycling in soil (Dungait et al. 2012). Partitioning the DOM into hydrophilic and hydrophobic compounds, which have distinct physicochemical properties and microbial availability, helps to clarify the protection mechanisms of soil organic matter (SOM) (Baumann et al. 2009). Generally, hydrophilic organic compounds (e.g., simple sugars, carboxylic acids, and amino acids) are highly available to soil microorganisms (Gunina et al. 2014; Gunina and Kuzyakov 2015; Straathof et al. 2014). That is, partly owing to that microbial transportation of hydrophilic organic compounds from extracellular to intracellular space requires less energy than that of hydrophobic organic compounds (Brant et al. 2006; Di Lonardo et al. 2017; Kalbitz et al. 2003a). In contrast, hydrophobic compounds (e.g., lignin and lipid) are less available, since that their hydrophobic property prevents the access by degradation enzymes and microorganisms (Rouse et al. 1994; Song et al. 2013) as well as passive movement in soil. Besides, the stronger sorption interaction with mineral surfaces (Kleber et al. 2007) makes hydrophobic compounds more resistant to biodegradation and consequently contributes to the stable SOM fractions (Kalbitz et al. 2003b; Song et al. 2013; Spaccini et al. 2002). Therefore, hydrophilicity and hydrophobicity of DOM are essential to illustrate the mechanisms of SOM stability.

The DOM input in soil via root exudates and plant residues change the turnover of native SOM, which is termed as priming effect (PE) (Jenkinson et al. 1985; Kuzyakov et al. 2000). PE can be positive, when the addition of DOM increases the mineralization of native SOM, or negative, when the DOM addition decreases the mineralization of native SOM (Fan et al. 2020; Kuzyakov 2010). The intensity and direction of PE vary with the physicochemical properties of inputs, which relate to C availability for microbes (Di Lonardo et al. 2017; Wang et al. 2020). The input of fresh organic matter with higher microbial availability generally induces stronger PE (Blagodatskaya and Kuzyakov 2008). For instance, a higher PE was observed with the addition of glucose than cellulose (Tian et al. 2019). In comparison, an opposite result was detected that hydrophobic compounds (cinnamic acid and stearic acid) induced stronger positive PE than those of hydrophilic compounds (glucose and starch) (Jagadamma et al. 2014). As

compared with these single and simple substrates, the hydrophilic and hydrophobic DOM contains more diverse and complex components (Gregorich et al. 2003; Qiu et al. 2015, 2016). Hence, PEs induced by the hydrophilic and hydrophobic DOM cannot be accurately predicted.

As the two main decomposers, bacteria and fungi are characterized by their fast-growing and slow-growing strategies, and thus considered as r- and K-strategists, respectively (Jagadamma et al. 2014; Reznick et al. 2002; Rousk and Bååth 2011). Both r- and K-strategists contribute to the mineralization of fresh organic substrates and their evoked PEs (Chen et al. 2014; Fontaine et al. 2003). According to the "stoichiometric decomposition" theory, r-strategists benefit from the utilization of highly available substrates and increase CO_2 efflux by accelerating microbial turnover (Chen et al. 2014; Hessen et al. 2004). Based on the "microbial N mining" theory, K-strategists have an advantage in utilizing recalcitrant organics, and thereby enhance SOM mineralization to satisfy the microbial demand for N (Chen et al. 2014; Kuzyakov et al. 2000). Hence, the intensity of mineralization and PEs involved by r-strategists could be stronger than that caused by K-strategists. Regarding the input of hydrophilic and hydrophobic substrates, nonetheless, clear experimental proof for the above-mentioned mechanisms that occur in soils is missing.

In the present study, we aimed to quantify the discrepancies in the mineralization of hydrophilic and hydrophobic fractions of DOM and induced PE in soils, and to clarify the underlying mechanisms driven by bacteria and fungi. ^{13}C-labelled hydrophilic and hydrophobic fractions extracted from maize plant residues were added into two typical cropland soils, i.e., well-drained upland and water-logged paddy soils. Since flooding inhibits microbial activities, especially for aerobic fungi (Xia et al. 2019), the contrasting discrepancy of microbial community in both soils is an ideal condition to test the functional groups involved in substrates degradation. Three hypotheses were evaluated: (1) the mineralization of the hydrophilic fraction and its PE will be faster and stronger than that of the hydrophobic fraction; (2) the mineralization and PE evoked by the addition of hydrophilic fraction are dominated by bacteria whereas fungi are mainly responsible for those induced by the hydrophobic fraction, since the r-strategists have a competitive advantage over K-strategists for highly available substrates (Blagodatskaya and Kuzyakov 2013; Reznick et al. 2002); (3) the mineralization and PE of both fractions will be weaker in paddy than in upland soils, owing to the suppression of microbial activity caused by oxygen limitation (Qiu et al. 2017).

Materials and methods

Field site and soil collection

Surface soils (0–15 cm depth) were collected from an upland field (24°56′37.6″N, 108°4′9.8″E) and a paddy field (24°57′41.2″N, 108°3′1.3″E) in Changde, Hunan Province, China, in July 2016. These soils are classified as Ultisol. Both croplands have been continuously cultivated for more than 20 years with two-season rotation of cotton and canola for upland and double rice for paddy. After harvest, plant residues were generally incorporated into the fields. Fresh soils were homogenized and sieved (< 2 mm); visible roots, plant residues, and rocks were removed, and samples were stored at 4 °C until use. The upland and paddy soils had the following properties: pH (H_2O) of 5.4 and 6.7, soil organic C of 14.7 and 19.3 g kg^{-1}, total N of 2.0 and 2.1 g kg^{-1}, and microbial biomass C of 235 and 595 mg kg^{-1}, clay of 13% and 9%, silt of 79% and 72%, and sand of 8% and 19%. The background $\delta^{13}C$ values of the upland and paddy soils were − 14.1‰ and − 20.2‰, respectively.

Production of ^{13}C-labelled substrates

Maize (Zea mays L.) seedlings were grown to maturity in a greenhouse labeling chamber with $^{13}CO_2$ (Ge et al. 2017). After 60 days, the aboveground plant biomass was harvested and dried at 60 °C. The maize plant contained 44.9% C and 1.97% N with $\delta^{13}C$ value of 1762‰. The hydrophilic and hydrophobic fractions were extracted according to the method described by Miao et al. (2017). In detail, the maize residue was minced and grounded to approximately 0.2 to 0.5 mm. A portion of the residue was subjected to extraction with double distilled water (1:20 w/v) at 80 °C for 5 h, cooled to room temperature, centrifuged at 7104×g for 10 min, and filtered through glass fiber filters (Advantec GB-140). This extraction process was performed twice to collect the hydrophilic (Hi) fraction. Following the same extraction process, another portion was extracted with hexane instead of double distilled water for 8 h using the Soxhlet extraction apparatus to collect the hydrophobic (Ho) fraction. Quartz sand was used as a carrier to deliver the extracted organic fractions into soils. Before use, the quartz sand was treated in a muffle furnace at 1000 °C for 24 h to remove C. In a fume hood, 160 g quartz sand (60 mesh) was mixed with 200 mL Hi or Ho fraction using a spatula in a 500-mL beaker. To ensure a uniform coating of organic fraction on the sand and remove hexane, the mixtures were evaporated to dryness with continuous mixing in a fume hood at room temperature via stirring for 2 min every half hour.

Total contents of C, N, and $\delta^{13}C$ value of the fraction-coated sands were analyzed using a stable isotope mass spectrometer (MAT 253; Thermo Scientific, Waltham, MA, USA). The Hi and Ho fractions in sand had the following properties: total C content of 0.77% and 0.43%, C:N ratio of 3.75 and 4.54, and $\delta^{13}C$ value of 1584‰ and 1357‰, respectively.

The chemical constituents of the Hi and Ho fractions were measured by gas chromatography-mass spectrometry (GCMS-QP2010 Shimadzu, Kyoto, Japan) (Zhou et al. 2010). The Hi and Ho fractions contained 6.3% and 2.8% alcohols, 0.9% and 8.9% aldehydes, 7.7% and 14.5% ethers, and 29.8% and 34.3% fatty acid methyl esters, respectively. Besides, the Hi fraction exclusively contained 15.3% alkanes, 7.7% aromatics, 5.1% amides, 15.0% ecanoic acid methyl ester, 7.2% fatty acids, 2.2% glycosides, and 2.9% miazines, while the Ho fraction exclusively contained 38.5% alkenes and 1.0% ketones.

Incubation experiment

Moist soil samples were pre-incubated at 25 °C for 14 days. Three treatments were established for each soil with four replicates: (1) soil without additions (control); (2) soil mixed with Hi fraction (Hi); (3) soil mixed with Ho fraction (Ho). Moist soil (50 g dry weight equivalent) was placed into flat tubes (40 mm, 120 mm height), and mixed with specific Hi or Ho fraction-coated sand mixtures at 150 mg C kg^{-1} soil. Additional sand without fraction coating was added to reach a final soil to sand mass ratio of 5%, such that equal amounts of sand were added to all treatments. Control soils were prepared in parallel with quartz sand lacking coated substrates. Samples were placed in 1-L jars and incubated in the dark at 25 °C for 40 days. All jars were sealed with a rubber plug. During incubation, upland soil was maintained under 45% water holding capacity, and paddy soil under the flooding condition (2 cm depth of water) with a supplement of distilled water. For each jar, 2 mL of distilled water was added to the bottom to maintain the air saturated humidity conditions.

Mineralization of added organic fractions and native SOM was quantified based on CO_2 emissions. To determine the evolution of CO_2 and its $\delta^{13}C$, two headspace gas samples were collected from each jar at 0.25, 1, 2, 3, 5, 10, 15, 20, 25, 30, 35, and 40 days. The gas was taken using a 30-mL syringe and injected into separate pre-evacuated 12-mL vacuum bottles fitted with butyl-rubber lids. After gas sampling, the jars were opened for aeration for 30 min. Another experiment was conducted with the similar conditions to measure the fraction-derived C incorporation into microbial biomass. Soil samples were destructively collected at 2, 7, and 40 days for the analysis of phospholipid fatty acids (PLFAs).

Analysis and calculation of CO_2

The CO_2 concentrations were analyzed using a gas chromatograph (Agilent 7890A; Agilent Technologies, Santa

Clara, CA, USA), equipped with a flame ionization detector for CO_2 analyses at 250 °C. The $\delta^{13}C$ in CO_2 was determined using an ultra-high-resolution isotope ratio mass spectrometer (MAT 253; Thermo Scientific, Waltham, MA, USA) coupled with a Gas Bench system (Thermo Scientific, Waltham, MA, USA)

The efflux rates of CO_2 derived from native SOM (Q_{SOM}, mg kg^{-1} day^{-1}) and the added fraction ($Q_{fraction}$, mg kg^{-1} day^{-1}) at each sampling time were calculated according to the following equations (Guenet et al. 2010; Wang et al. 2019):

$$Q_{SOM} = Q_{total} \times \frac{(\delta_{fraction} - \delta_{total})}{(\delta_{fraction} - \delta_{control})} \tag{1}$$

$$Q_{fraction} = Q_{total} - Q_{SOM} \tag{2}$$

where δ_{total} and $\delta_{control}$ represent $\delta^{13}C$ values of CO_2 production from samples with and without fraction addition, respectively; $\delta_{fraction}$ is the $\delta^{13}C$ value of the added fraction; Q_{total} is the total CO_2 flux from soils with fraction addition.

Cumulative production of SOM-derived CO_2 (T, mg kg^{-1}) was calculated by the following equation (Chao et al. 2019):

$$T_{SOM} = \sum_{i=1}^{n} \left[\frac{Q_i + Q_{i+1}}{2} \times (t_{i+1} - t_i) \right] \tag{3}$$

where Q_i and Q_{i+1} represent the release rate of soil-derived CO_2 efflux at ith and $(i+1)$th incubation time, respectively; $t_{i+1} - t_i$ is the interval between the ith and $(i+1)$th incubation time (d); n is the number of sampling times.

The cumulative PE was calculated according to the following equation:

$$PE = T_{SOM} - T_{control} \tag{4}$$

where $T_{control}$ is the cumulative CO_2 production (mg kg^{-1}) in soils without fraction addition.

Analysis and calculation of PLFAs

Soil microbial PLFAs were analyzed according to methods described by Yuan et al. (2016). Briefly, lipids were extracted twice from 2 g of finely ground freeze-dried samples using 22.8 mL one-phase chloroform/methanol/citrate buffer system (1:2:0.8 v/v/v; pH 4.0) and were separated using silica acid columns (Supelco, Bellefonte, PA, USA). The phospholipids were subjected to mild alkaline methanolysis. Then, fatty acid methyl esters were identified based on their relative retention times on gas chromatography (Agilent 7890A; Agilent Technologies, Santa Clara, CA, USA) and were quantified using methyl nonadecanoate (19:0) as an internal standard. $\delta^{13}C$ values of individual PLFAs were analyzed using a Trace GC Ultra gas chromatograph (Thermo Electron Corp., Milan, Italy)

with a combustion column attached via GC Combustion III to a Delta V Advantage isotope ratio mass spectrometer (IRMS; Thermo Finnigan, Bremen, Germany).

$\delta^{13}C$ values of each PLFA molecule were corrected for the C added during derivatization using the following mass balance equation:

$$n_{cd}\delta^{13}C_{cd} = n_c\delta^{13}C_c + n_d\delta^{13}C_d \tag{5}$$

where n is the number of C atoms, c is the compound of interest, d is the derivatizing agent (methanol: $n_d = 1$ and $\delta^{13}C_d = -29.33‰$), and cd is the corresponding derivatized compound of interest (Dungait et al. 2011; Wang et al. 2014).

Fraction-derived C in individual PLFAs (P_i; μg C kg^{-1} soil) was quantified using the following equation:

$$P_i = C_i \times (\delta^{13}C_c - \delta^{13}C_{control}) / (\delta_{fraction} - \delta_{control}) \tag{6}$$

where C_i is the C content (μg C kg^{-1} soil) of the individual PLFAs. $\delta^{13}C_c$ is the corrected $\delta^{13}C$ value of each PLFA in soils with fraction addition and $\delta^{13}C_{control}$ is the corresponding $\delta^{13}C$ value of individual PLFAs without addition.

The fatty acids i15:0, a15:0, i16:0, 16:1ω7c, 10Me16:0, 10Me17:0, 10Me18:0, a17:0, i17:0, cy17:0, 18:1ω7c, and cy19:0 were used as biomarkers for bacteria (Moore-Kucera and Dick 2008). The fatty acid of 18:1ω9c was regarded as indicator of fungi (Bååth and Anderson 2003; Frostegård et al. 1993). Total fraction-derived C in bacterial or fungal groups (P_t; μg C kg^{-1} soil) was calculated according to the following equation:

$$P_t = \sum P_i \tag{7}$$

The total PLFAs content was calculated as the sum of bacterial and fungal PLFAs. The microbial use efficiency of fraction-derived C (fraction-CUE) was calculated as the fraction-derived C incorporated into PLFAs relative to its total consumption (including respiration and incorporation into microbial PLFAs) (Hicks et al. 2019). The turnover rate (% day^{-1}) of the PLFAs at each sampling time was calculated using the following equation (Schneckenberger and Kuzyakov 2007):

$$\text{Turnover rate} = -ln(1 - \text{Proportion}_{PLFAs}) / \text{Time} \tag{8}$$

where $\text{Proportion}_{PLFAs}$ represents the proportion of fraction-derived PLFAs in total PLFAs, and Time represents incubation time (day).

Statistical analyses

The differences of the fraction or SOM-derived CO_2 efflux rate, cumulative fraction-derived CO_2 efflux, and cumulative PE among treatments were tested using ANOVA with

repeated measurements. Independent-samples t test was used to evaluate the difference between treatments with Hi and Ho fractions addition at each sampling time. Homogeneity of variances was tested by Levene's test; normal distribution of residues was tested by the Shapiro test. Differences were considered significant at $p < 0.05$ followed by Duncan's test. The above analyses were conducted for the upland and paddy soils separately. All statistical analyses were performed using SPSS Windows version 18.0 (SPSS Inc., Chicago, USA). Principal component analysis (PCA) was performed based on the PLFAs data after $\log_e$ transformation using CANOCO 5.0 for Windows (Microcomputer Power, Ithaca, NY, USA). Figures were generated using Origin Lab 2017.

Results

Mineralization of hydrophilic and hydrophobic fractions

Repeated measures ANOVA showed significant effects of fraction type, time and their interactions on the mineralization rate and the cumulative mineralization of the added fractions ($p < 0.05$; Fig. 1). There is an exception that fraction type in paddy soil did not significantly affect the cumulative mineralization (Fig. 1d). At the early incubation stage (6–24 h), the mineralization rates of Hi fraction were 3.6–36 and 3.8–55.3 times faster than those of Ho fraction in upland and paddy

soils, respectively ($p < 0.05$; Fig. 1a, b). Thereafter, the mineralization of Ho fraction was significantly faster than that of Hi fraction until day 40 and 14 in upland and paddy soils, respectively ($p < 0.05$). At the end of incubation, the cumulative mineralization of Hi and Ho fractions was similar in each soils ($p > 0.05$). Remarkably, the mineralization rate reached a maximum sooner for Hi fraction (at 6 and 24 h in upland and paddy soils, respectively) than that for Ho fraction (at day 3 in both soils).

During incubation, mineralization of both fractions was faster in upland than in paddy soil. At the end of incubation, cumulative fraction-derived CO_2 release from the upland (132.7–143.7 mg kg^{-1}) was larger than that from paddy soil (49.4–54.5 mg kg^{-1}) (Fig. 1c, d).

Priming effect

Significant effects of fraction type on both SOM-derived CO_2 efflux rate and cumulative PE were observed in upland ($p < 0.05$) but not in paddy soils ($p > 0.05$) (Fig. 2). Incubation time had significant effects on these indices in both soils ($p < 0.05$). Significant interaction effects from fraction type and incubation time were only observed for the SOM-derived CO_2 efflux rate in upland soil (Fig. 2a). At the early incubation stage (6–24 h), the PEs evoked by Hi fraction were 5.7–10.1 times and 1.5–6.5 times greater than that by Ho fraction in upland and paddy soils, respectively ($p < 0.05$, Fig. 2c, d). At the end of incubation, however, the cumulative

Fig. 1 CO_2 efflux rate and cumulative CO_2 derived from ^{13}C-labelled hydrophilic and hydrophobic fractions in upland and paddy soils. Hi, hydrophilic fraction; Ho, hydrophobic fraction. Data are expressed as means ± SD ($n = 4$). *, significant difference between Hi and Ho treatments. The y-axis scale in paddy is smaller than in upland
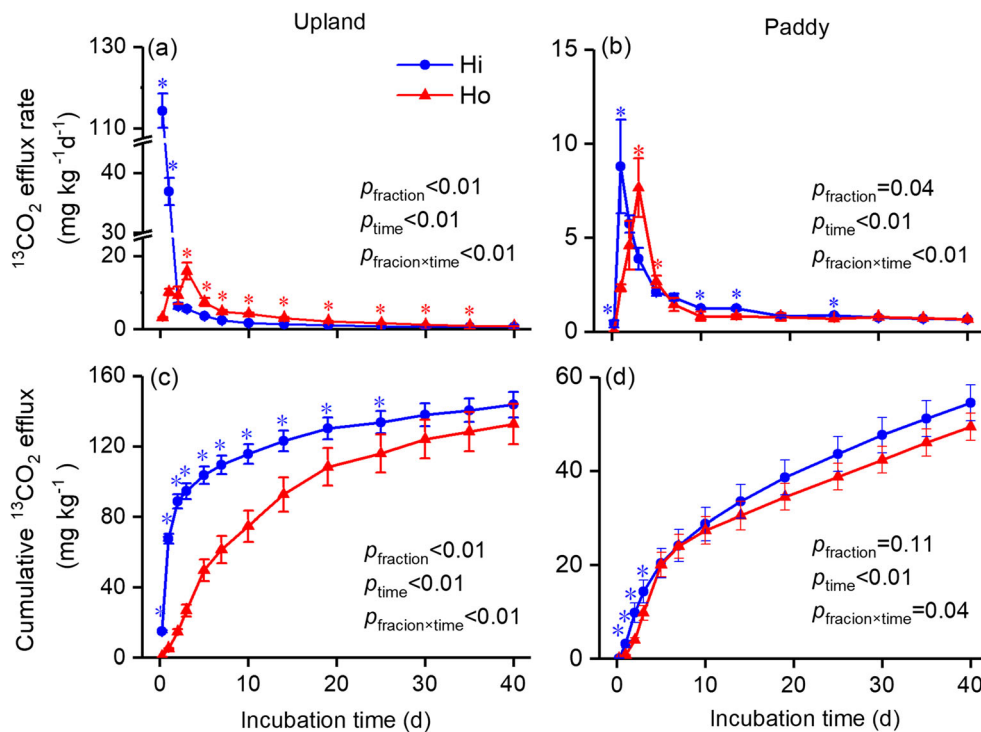
Fig. 2 SOM-derived CO_2 efflux rate and cumulative PE with the addition of hydrophilic and hydrophobic fractions in upland and paddy soils. Hi, hydrophilic fraction; Ho, hydrophobic fraction. Data are expressed as means ± SD ($n = 4$). *, significant difference between Hi and Ho treatments. The y-axis scale in paddy is smaller than in upland
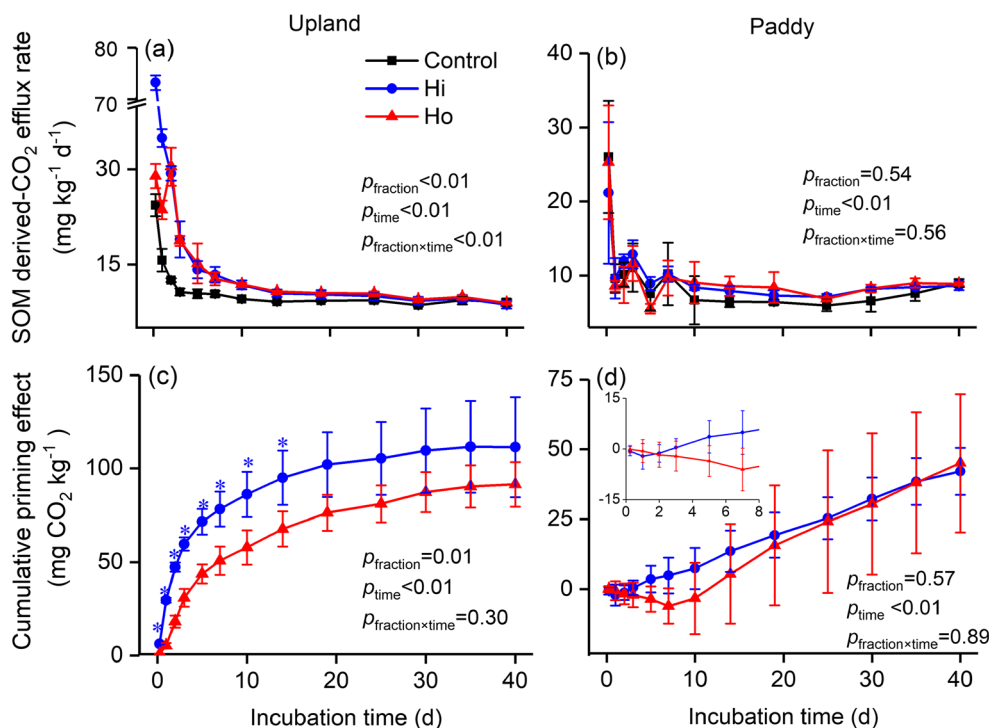

PEs induced by Hi and Ho fractions were similar, owing to the marginally greater PE induced by Ho fraction than Hi fraction after 24 h (Fig. 2a, b). In upland soil, the addition of both fractions increased the release rate of SOM-derived CO_2 by 2–195% until day 20 as compared with control (Fig. 2a), leading to a positive PE (Fig. 2c). In paddy soil, however, both fractions addition decreased SOM-derived CO_2 efflux rate by 2–19% at the early stage (Fig. 2b), resulting in a negative PE within 2 and 10 days for Hi and Ho additions, respectively (Fig. 2d). At the end of incubation, the PEs evoked by the Hi and Ho fractions in upland soil were 2.2–2.4 times higher than those in paddy soil (Fig. 2c, d).

Incorporation of hydrophilic and hydrophobic fractions-derived C into PLFAs

During incubation, the incorporation of the Hi-derived C into bacterial PLFA was generally larger than that of the Ho-derived C in both soils ($p < 0.05$, Fig. 3a, b). The amount of fungal PLFAs with C derived from the Ho fraction was greater than that derived from the Hi fraction ($p < 0.05$, Fig. 3a, b). Bacteria accounted for 93–95% and 38–74% of the total microbial utilization of the Hi and Ho fractions, respectively. The amount of Hi- and Ho-derived C in total PLFAs in upland soil

Fig. 3 Incorporation of fraction-derived ^{13}C into bacterial and fungal PLFA in upland and paddy soil. Hi, hydrophilic fraction; Ho, hydrophobic fraction. Data are expressed as means ± SD ($n = 4$). The percentage of ^{13}C labelled bacterial PLFAs in total ^{13}C-PLFAs (%) was presented inside the bars. *, significant difference between Hi and Ho fractions-derived C in a same microbial PLFA. #, significant difference of total ^{13}C-PLFA between upland and paddy. The y-axis scale in paddy is smaller than in upland
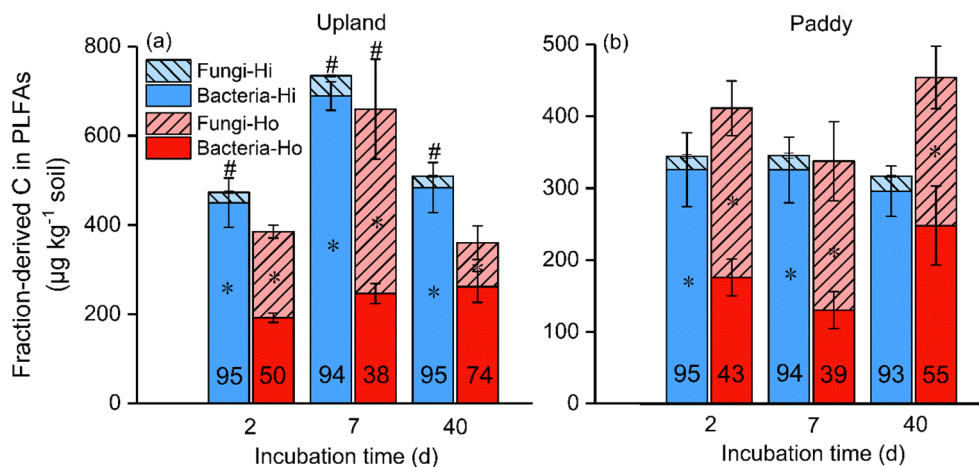
was 1.4–2.1 and 0.8–1.9 times than that in paddy soil, respectively.

The fraction type, incubation time, and their interactions significantly affected microbial CUE in both soils ($p < 0.05$) (Fig. 4a, b). The CUE of Ho fraction was 1.0–2.9 times larger than that of Hi fractions in both soils. As a whole, the differences of CUE between both fractions reduced with the decrease of CUE over the incubation. The microbial CUE of both factions was greater in paddy than that in upland soil.

At the early stages (2 and 7 days), the turnover rate of bacterial ^{13}C-PLFAs derived from Hi fraction was 1.7–2.5 times faster than those derived from the Ho fraction. An opposite trend was observed for the fungal ^{13}C-PLFAs with 7.4–13.0 times faster for the Ho fraction than Hi fraction. These differences in ^{13}C-PLFAs derived from Hi and Ho fractions decreased by the end of incubation (Fig. 5a, b). The turnover rates of bacterial and fungal ^{13}C-PLFAs were 1.1–4.1 times faster in upland than paddy soil (Fig. 5a, b).

In both soils, the composition of microbial PLFAs derived from the Hi fraction was separated from the Ho fraction along PC1, which explained 55.3–69.2% of the total variance (Fig. 6a, b). There was much less separation of PLFA compositions with incubation time along PC2 (explained 11.2–14.8%) compared with the separation according to substrate type (Fig. 6a, b). The PLFA compositions were separated more along PC2 in upland than paddy soil (Fig. 6a, b).

Discussion

Mineralization of hydrophilic and hydrophobic organic fractions

The faster mineralization of hydrophilic fraction than hydrophobic fraction in both soils supports our first hypothesis, although this phenomenon was only observed at the early incubation stage. This could be attributed to the following reasons. First, the greatly differed chemical composition of the extracted fractions leads to their contrasting

stability. The hydrophilic fraction exclusively contained the labile nitrogen-containing compounds (e.g., amides, amino acids, miazines, DAMEs, and FAMEs, accounting for 26.9% of the total amount), alkanes (15.3%), and glycosides (2.2%) because of their hydrolytic bonds (Dungait et al. 2012; von Lüetzow et al. 2006). By contrast, the hydrophobic fraction exclusively contained recalcitrant compounds (e.g., alkenes, 38.5%) because of their non-hydrolytic bonds (Lorenz et al. 2007; Xu et al. 2017). Second, the uptake of hydrophilic fraction was predominated by bacteria, whereas fungi preferred hydrophobic fraction. This finding was supported by that at day 2, the amount of hydrophilic fraction incorporated into bacteria was 11.4–16.4 times greater than that into fungi, whereas the amount of hydrophobic fraction incorporated into fungi was 1.0–1.5 times larger than that into bacteria (Fig. 3a, b). The microbial CUE of hydrophilic fraction was lower than that of hydrophobic fraction (Fig. 4a, b) because fungi have higher biomass ratios of C:N and will allocate more C to biomass per unit of substrate used than bacteria (Soares and Rousk 2019). Meanwhile, the consumption of organic substrates by r-strategists (bacteria) is faster than that by K-strategists (fungi) (Geyer et al. 2016; Rousk and Bååth 2011). Therefore, the rate of $^{13}CO_2$ release from hydrophilic fraction is greater and faster than that from hydrophobic fraction (Fig. 1a, b).

At the end of incubation, the cumulative mineralization of hydrophilic and hydrophobic fractions, either in upland or in paddy soils, were similar (Fig. 1c, d). This result is explained by the opposite trends of mineralization rates of both fractions between the early and late incubation stages. That is, the mineralization of hydrophobic fraction was more rapid than that of hydrophilic fraction after day 2 in upland soil and from day 3 to 5 in paddy soil (Fig. 1a, b) because of the shifts of bacteria and fungi (Figs. 3a, b and 6a, b) (Collins et al. 2016). According to the r- and K-selection theory, fast-growing bacteria predominate the decomposition of added substrates at the early stage (Kuzyakov 2010; Reznick et al. 2002). Then, slow-

Fig. 4 Microbial C use efficiency (^{13}C incorporation in PLFAs relative to the sum of ^{13}C incorporation in PLFAs and ^{13}C released as CO_2) of hydrophilic (Hi) and hydrophobic (Ho) fractions in upland and paddy soils. Data are expressed as means ± SD ($n = 4$). *, significant difference between Hi and Ho treatments. #, significant difference between upland and paddy soils. The y-axis scale in upland is smaller than in paddy
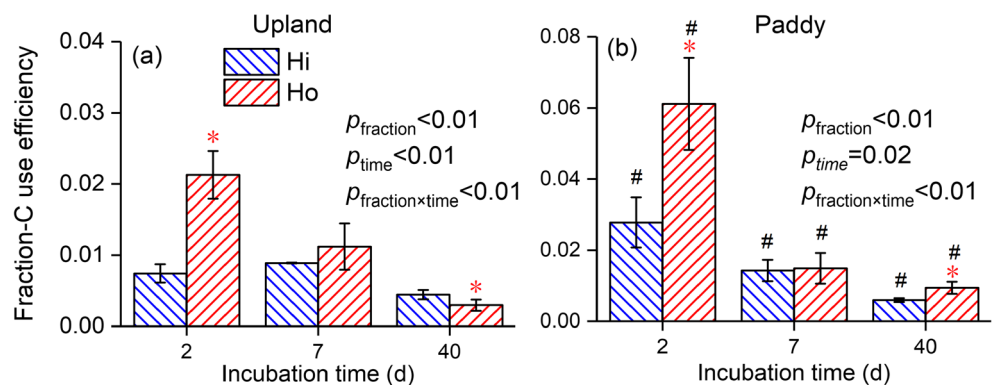
Fig. 5 Turnover rate of bacterial and fungal PLFAs derived from hydrophilic (Hi) and hydrophobic (Ho) fractions in upland and paddy soils at 2, 7, and 40 days. Data are expressed as means ± SD (n = 4). *, significant difference between Hi and Ho treatments. #, significant difference between bacteria and fungi for Hi-added treatment; $, significant difference between bacteria and fungi for Ho-added treatment. The y-axis scale in paddy is smaller than in upland
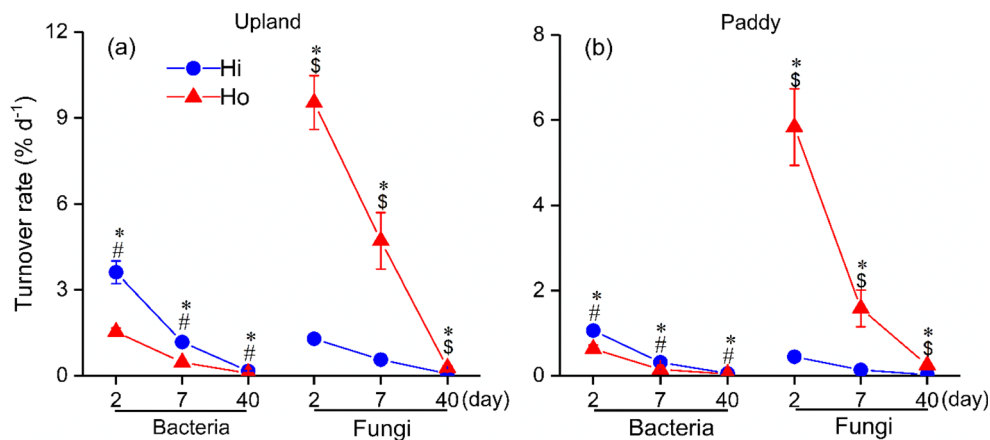
growing fungi gradually prevail because the exhaustion of available C leads to the death of fast-growing bacteria (Jagadamma et al. 2014; Shahbaz et al. 2017). Therefore, the preference for the bacterial uptake of hydrophilic fraction and fungal utilization of hydrophobic fraction resulted in a greater decrease in the decomposition of hydrophilic fraction than hydrophobic one in the later stage (Fig. 3a, b), which finally leads to similar cumulative mineralization.

Hydrophobicity of organic substrates could limit their accessibility to microorganisms or enzymes (Dungait et al. 2012; von Lüetzow et al. 2006). However, our results demonstrate a rapid uptake of hydrophobic fraction by fungi as indicated by their initial turnover rates (Fig. 5a, b). It should be noted that the preferential uptake of hydrophilic and hydrophobic compounds by bacteria and fungi, respectively (Fig. 3a, b), could lead to their divergent fates via the various microbial metabolic pathways (Ma et al. 2018; Soares and Rousk 2019). Specifically, the longer residence time of fungal biomass (130–150 days) than that of bacteria (2.3–33 days) (Gunina et al. 2017; Rousk and Bååth 2007) may lead to a greater contribution from the hydrophobic fraction to C accumulation in the form of microbial residues (Liang et al. 2017; Xia et al. 2019).

Priming effect of hydrophilic and hydrophobic fractions

PE can be classified as real or apparent based on the origin of the extra CO_2 released from the soil (Blagodatskaya and Kuzyakov 2011; Di Lonardo et al. 2017). Jenkinson et al. (1985) suggested that real PE is an increase in the decomposition of recalcitrant SOM, whereas apparent PE is an increase of microbial C turnover, which is not linked with changes of SOM decomposition. With the input of fresh C, real and apparent PEs occur simultaneously and cannot be disentangled in our study (Blagodatskaya and Kuzyakov 2011; Blagodatsky et al. 2010). Since both real and apparent PEs are governed by microbial activity, the intensity and direction of PE can be evaluated by the succession of microbial community composition, especially by distinguishing the bacteria and fungi with contrasting growth strategies (Blagodatsky et al. 2010).

In the present study, hydrophilic fraction induced stronger PE than hydrophobic fraction at the initial stage, although their cumulative PE at the end of incubation was similar (Fig. 2c, d). The discrepancy in the dynamics of PE caused

Fig. 6 Principal component analysis (PCA) of PLFAs compositions with ^{13}C derived from hydrophilic (Hi) and hydrophobic (Ho) fractions in upland and paddy soils at 2, 7, and 40 days. Arrows indicate the effect of incubation time
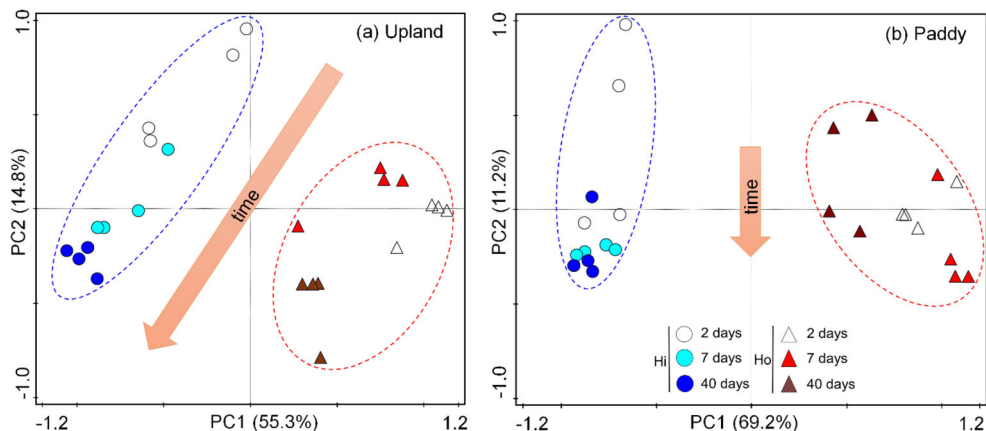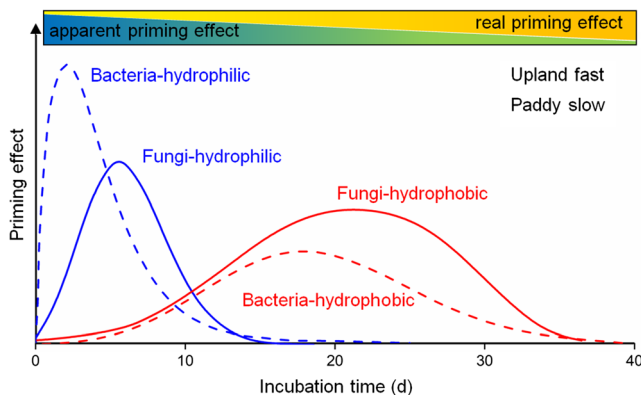
by hydrophilic and hydrophobic fractions can be linked to the apparent and real PE dominated by bacteria and fungi, respectively, through the following process chain (Fig. 7):

(1) Most soil microorganisms are dormant due to limited C availability (Dungait et al. 2011; Farrell et al. 2014; Mondini et al. 2006). The addition of fresh organic substrates results in shifts in both bacteria and fungi from dormant to active states (De Nobili et al. 2001), as evidenced by the increase in microbial biomass (Figs. 3a, b and S1), microbial growth, and respiration (Blagodatskaya et al. 2014). The activated microbial community switches to the utilization of the available specific compounds from added hydrophilic and hydrophobic fractions (Blagodatskaya and Kuzyakov 2013; Kuzyakov et al. 2000).

(2) Among the activated microorganisms, bacteria (dominated by r-strategists) feeding on fresh available substrates grow more quick than fungi (dominated by K-strategists) feeding on refractory fresh and native organic matter (Blagodatsky et al. 2010; Fontaine et al. 2003, 2011). This leads to a faster biomass turnover of bacteria than fungi (Gunina et al. 2017). Therefore, the PE evoked by bacteria is dominated by apparent PE (occurs fast but lasts for a short time). By contrast, PE evoked by fungi is dominated by real PE (occurs slow but lasts for a long time) (Blagodatsky et al. 2010; Kuzyakov 2010). In the present study, hydrophilic and hydrophobic fractions were utilized by both bacteria and fungi (Fig. 3a, b). However, incorporation of hydrophilic fraction into bacteria was greater than that integrated into fungi, especially at the initial stage, while the opposite trend was

observed for hydrophobic fraction (Fig. 3a, b). Hence, the preferential uptake of hydrophilic fraction by bacteria triggers stronger apparent PE than the preferential uptake of hydrophobic fractions by fungi (Fig. 7).

(3) After the consumption of easily available substrates (the $^{13}CO_2$ efflux rate decreased sharply, Fig. 1a, b), the r-strategists die, as evidenced by the decrease of bacterial ^{13}C-PLFAs from day 7 to 40 (Fig. 3a, b). Thus, the apparent PE mainly derived from bacteria will decrease during the incubation and the real PE mainly induced by fungi will increase (Kuzyakov 2010; Qiao et al. 2019; Shahbaz et al. 2018). This will reduce the gap in cumulative PE between hydrophilic and hydrophobic fractions (Figs. 2c, d and 7) and the divergence of their effects on the composition of main microbial group and SOM turnover.

Comparisons between upland and paddy soils

The delay in the maximum mineralization rate of hydrophilic and hydrophobic fractions in paddy than in upland soils (Fig. 1a, b) reflects the slower C transformation due to oxygen limitation (Sun et al. 2015). Although the microbial biomass pool is larger in paddy soil, the low oxygen condition caused by flooding limits the activity of aerobic microorganisms, especially for fungi (Xia et al. 2019). This was evidenced by the higher amount of fungal PLFA but lower fungal ^{13}C-PLFA in paddy soil as compared to upland soil (Figs. 3a, b and S1). Besides, the flooding condition may oblige microorganisms to divert C resources from reproduction to survival (Qiu et al. 2017), resulting in slower mineralization.

Less mineralization from native SOM in soil with substrate addition compared to control soil, i.e., negative PE, is generally attributed to the fact that most soil microbes preferentially utilize fresh labile substrates relative to old native SOM (Fan et al. 2020; Fontaine et al. 2003). However, the negative PE was only detected in paddy soil but not in upland soil (Fig. 2c, d). This is attributed to the fact that the first sampling time was 6 h after substrate addition. By that time, the negative PE may be missed because the response of microbes to the addition of easily utilizable substrates is very quick and persists for less than a few hours (Stenström et al. 2001). The negative PE was observed in flooding paddy soil, owing to the slower response of microbes to fresh substrates under anaerobic conditions (Kögel-Knabner et al. 2010).

Fig. 7 A conceptual overview of the priming effect (PE) evoked by bacteria and fungi in soils with the addition of hydrophilic and hydrophobic fractions. The dash or solid lines represent the total PE (including both apparent and real PE) induced by bacteria or fungi, respectively. The blue or red lines represent the hydrophilic or hydrophobic additions, respectively. The rectangle at the top was divided into green and yellow parts to represent the apparent PE or real PE induced by both bacteria and fungi, respectively. Time points in this figure represented the example in upland soil. PE is slower in paddy soil than in upland soil

Conclusions

Our findings demonstrated that the processes of the mineralization and PE of hydrophilic and hydrophobic dissolved

organic matter are divergent in soils and are driven by specific groups of microbial community. In the initial stage, the hydrophilic fraction of plant residues had faster mineralization rate and induced stronger PE compared with hydrophobic fraction. The higher mineralization of hydrophilic fraction than hydrophobic one was attributed to the preferences of r-strategists (fast-growing bacteria) for the uptake of hydrophilic fraction and K-strategists (slow-growing fungi) for utilizing hydrophobic fraction. As compared with K-strategists, the r-strategists triggered stronger apparent PE by accelerating microbial biomass turnover, resulting in the stronger PE for hydrophilic fraction than hydrophobic one. This specific uptake of hydrophilic and hydrophobic compounds will ultimately affect the long-term formation, stabilization, and destabilization (e.g., by priming) of soil organic matter.

Compliance with ethical standards

Conflict of interest The authors declare that they have no conflict of interest.

References

Bååth E, Anderson TH (2003) Comparison of soil fungal/bacterial ratios in a pH gradient using physiological and PLFA-based techniques. Soil Biol Biochem 35:955–963

Baumann K, Marschner P, Smernik RJ, Baldock JA (2009) Residue chemistry and microbial community structure during decomposition of eucalypt, wheat and vetch residues. Soil Biol Biochem 41:1966–1975

Blagodatskaya E, Kuzyakov Y (2008) Mechanisms of real and apparent priming effects and their dependence on soil microbial biomass and community structure: critical review. Biol Fert Soils 45:115–131

Blagodatskaya E, Kuzyakov Y (2011) Priming effects in relation to soil conditions mechanisms. In: Gliński J, Horabik J, Lipiec J (eds) Encyclopedia of Agrophysics. Springer Netherlands, 2014, pp 657–667

Blagodatskaya E, Kuzyakov Y (2013) Active microorganisms in soil: critical review of estimation criteria and approaches. Soil Biol Biochem 67:192–211

Blagodatskaya E, Khomyakov N, Myachina O, Bogomolova I, Blagodatsky S, Kuzyakov Y (2014) Microbial interactions affect sources of priming induced by cellulose. Soil Biol Biochem 74:39–49

Blagodatsky S, Blagodatskaya E, Yuyukina T, Kuzyakov Y (2010) Model of apparent and real priming effects: linking microbial activity with soil organic matter decomposition. Soil Biol Biochem 42:1275–1283

Brant JB, Sulzman EW, Myrold DD (2006) Microbial community utilization of added carbon substrates in response to long-term carbon input manipulation. Soil Biol Biochem 38:2219–2232

Chen R, Senbayram M, Blagodatsky S, Myachina O, Dittert K, Lin X, Blagodatskaya E, Kuzyakov Y (2014) Soil C and N availability determine the priming effect: microbial N mining and stoichiometric decomposition theories. Glob Chang Biol 20:2356–2367

Chen X, Liu M, Kuzyakov Y, Li W, Liu J, Jiang C, Wu M, Li Z (2018) Incorporation of rice straw carbon into dissolved organic matter and microbial biomass along a 100-year paddy soil chronosequence. Appl Soil Ecol 130:84–90

Collins CG, Carey CJ, Aronson EL, Kopp CW, Diez JM (2016) Direct and indirect effects of native range expansion on soil microbial community structure and function. J Ecol 104:1271–1283

De Nobili M, Contin M, Mondini C, Brookes PC (2001) Soil microbial biomass is triggered into activity by trace amounts of substrate. Soil Biol Biochem 33:1163–1170

Di Lonardo DP, De Boer W, Klein Gunnewiek PJ, Hannula SE, Van der Wal A (2017) Priming of soil organic matter: chemical structure of added compounds is more important than the energy content. Soil Biol Biochem 108:41–54

Dungait JAJ, Kemmitt SJ, Michallon L, Guo S, Wen Q, Brookes PC, Evershed RP (2011) Variable responses of the soil microbial biomass to trace concentrations of ^{13}C-labelled glucose, using ^{13}C-PLFA analysis. Eur J Soil Sci 62:117–126

Dungait JAJ, Hopkins DW, Gregory AS, Whitmore AP (2012) Soil organic matter turnover is governed by accessibility not recalcitrance. Glob Chang Biol 18:1781–1796

Fan Y, Zhong X, Lin TC, Lyu M, Wang M, Hu W, Yang Z, Chen G, Guo J, Yang Y (2020) Effects of nitrogen addition on DOM-induced soil priming effects in a subtropical plantation forest and a natural forest. Biol Fert Soils 56:205–216

Farrell M, Prendergast-Miller M, Jones DL, Hill PW, Condron LM (2014) Soil microbial organic nitrogen uptake is regulated by carbon availability. Soil Biol Biochem 77:261–267

Fontaine S, Mariotti A, Abbadie L (2003) The priming effect of organic matter: a question of microbial competition? Soil Biol Biochem 35:837–843

Fontaine S, Henault C, Aamor A, Bdioui N, Bloor JMG, Maire V, Mary B, Revaillot S, Maron PA (2011) Fungi mediate long term sequestration of carbon and nitrogen in soil through their priming effect. Soil Biol Biochem 43:86–96

Frostegård Å, Bååth E, Tunlio A (1993) Shifts in the structure of soil microbial communities in limed forests as revealed by phospholipid fatty-acid analysis. Soil Biol Biochem 25:723–730

Ge T, Li B, Zhu Z, Hu Y, Yuan H, Dorodnikov M, Jones DL, Wu J, Kuzyakov Y (2017) Rice rhizodeposition and its utilization by microbial groups depends on N fertilization. Biol Fert Soils 53:37–48

Geyer KM, Kyker-Snowman E, Grandy AS, Frey SD (2016) Microbial carbon use efficiency: accounting for population, community, and ecosystem-scale controls over the fate of metabolized organic matter. Biogeochemistry 127:173–188

Gregorich E, Beare M, Stoklas U, St-Georges P (2003) Biodegradability of soluble organic matter in maize-cropped soils. Geoderma 113:237–252

Guenet B, Leloup J, Raynaud X, Bardoux G, Abbadie L (2010) Negative priming effect on mineralization in a soil free of vegetation for 80 years. Eur J Soil Sci 61:384–391

Gunina A, Kuzyakov Y (2015) Sugars in soil and sweets for microorganisms: review of origin, content, composition and fate. Soil Biol Biochem 90:87–100

Gunina A, Dippold MA, Glaser B, Kuzyakov Y (2014) Fate of low molecular weight organic substances in an arable soil: from microbial uptake to utilisation and stabilisation. Soil Biol Biochem 77:304–313

Gunina A, Dippold M, Glaser B, Kuzyakov Y (2017) Turnover of microbial groups and cell components in soil: ^{13}C analysis of cellular biomarkers. Biogeosciences 14:271–283

Hessen DO, Ågren GI, Anderson TR, Elser JJ, De Ruiter PC (2004) Carbon, sequestration in ecosystems: the role of stoichiometry. Ecology 85:1179–1192

Hicks LC, Meir P, Nottingham AT, Reay DS, Stott AW, Salinas N, Whitaker J (2019) Carbon and nitrogen inputs differentially affect priming of soil organic matter in tropical lowland and montane soils. Soil Biol Biochem 129:212–222

Jagadamma S, Mayes MA, Steinweg MJ, Schaeffer SM (2014) Substrate quality alters microbial mineralization of added substrate and soil organic carbon. Biogeosciences 11:4665–4467

Jenkinson DS, Fox RH, Rayner JH (1985) Interactions between fertilizer nitrogen and soil-nitrogen—the so-called priming effect. Eur J Soil Sci 36:425–444

Kalbitz K, Schmerwitz J, Schwesig D, Matzner E (2003a) Biodegradation of soil-derived dissolved organic matter as related to its properties. Geoderma 113:273–291

Kalbitz K, Schwesig D, Schmerwitz J, Kaiser K, Haumaier L, Glaser B, Ellerbrock R, Leinweber P (2003b) Changes in properties of soil-derived dissolved organic matter induced by biodegradation. Soil Biol Biochem 35:1129–1142

Kleber M, Sollins P, Sutton R (2007) A conceptual model of organo-mineral interactions in soils: self-assembly of organic molecular fragments into zonal structures on mineral surfaces. Biogeochemistry 85:9–24

Kögel-Knabner I, Amelung W, Cao Z, Fiedler S, Frenzel P, Jahn R, Kalbitz K, Kölbl A, Schloter M (2010) Biogeochemistry of paddy soils. Geoderma 157:1–14

Kuzyakov Y (2010) Priming effects: interactions between living and dead organic matter. Soil Biol Biochem 42:1363–1371

Kuzyakov Y, Friedel JK, Stahr K (2000) Review of mechanisms and quantification of priming effects. Soil Biol Biochem 32:1485–1498

Liang C, Schimel JP, Jastrow JD (2017) The importance of anabolism in microbial control over soil carbon storage. Nat Microbiol 2:17105

Lorenz K, Lal R, Preston CM, Nierop KGJ (2007) Strengthening the soil organic carbon pool by increasing contributions from recalcitrant aliphatic bio(macro)molecules. Geoderma 142:1–10

Ma T, Zhu S, Wang Z, Chen D, Dai G, Feng B, Su X, Hu H, Li K, Han W, Liang C, Bai Y, Feng X (2018) Divergent accumulation of microbial necromass and plant lignin components in grassland soils. Nat Commun 9:3480

Miao S, Ye R, Qiao Y, Zhu-Barker X, Doane TA, Horwath WR (2017) The solubility of carbon inputs affects the priming of soil organic matter. Plant Soil 410:129–138

Mondini C, Cayuela ML, Sanchez-Monedero MA, Roig A, Brookes PC (2006) Soil microbial biomass activation by trace amounts of readily available substrate. Biol Fert Soils 42:542–549

Moore-Kucera J, Dick RP (2008) Application of ^{13}C-labeled litter and root materials for in situ decomposition studies using phospholipid fatty acids. Soil Biol Biochem 40:2485–2493

Qiao N, Wang J, Xu X, Shen Y, Long Xe HY, Schaefer D, Li S, Wang H, Kuzyakov Y (2019) Priming alters soil carbon dynamics during forest succession. Biol Fert Soils 55:339–350

Qiu Q, Wu L, Ouyang Z, Li B, XuY WS, Gregorich EG (2015) Effects of plant-derived dissolved organic matter (DOM) on soil CO_2 and N_2O emissions and soil carbon and nitrogen sequestrations. Appl Soil Ecol 96:122–130

Qiu Q, Wu L, Ouyang Z, Li B, Xu Y (2016) Different effects of plantderived dissolved organic matter (DOM) and urea on the priming of soil organic carbon. Environ Sci Proc Imp 18:330–341

Qiu H, Zheng X, Ge T, Dorodnikov M, Chen X, Hu Y, Kuzyakov Y, Wu J, Su Y, Zhang Z (2017) Weaker priming and mineralisation of low molecular weight organic substances in paddy than in upland soil. Eur J Soil Biol 83:9–17

Reznick D, Bryant MJ, Bashey F (2002) r- and K-selection revisited: the role of population regulation in life-history evolution. Ecology 83:1509–1520

Rouse JD, Sabatini DA, Suflita JM, Harwell JH (1994) Influence of surfactants on microbial degradation of organic compounds. Crit Rev Environ Sci Technol 24:325–370

Rousk J, Bååth E (2007) Fungal biomass production and turnover in soil estimated using the acetate-in-ergosterol technique. Soil Biol Biochem 39:2173–2177

Rousk J, Bååth E (2011) Growth of saprotrophic fungi and bacteria in soil. FEMS Microbiol Ecol 78:17–30

Schneckenberger K, Kuzyakov Y (2007) Carbon sequestration under Miscanthus in sandy and loamy soils estimated by natural ^{13}C abundance. J Plant Nutr Soil Sci 170:538–542

Shahbaz M, Kuzyakov Y, Sanaullah M, Heitkamp F, Zelenev V, Kumar A, Blagodatskaya E (2017) Microbial decomposition of soil organic matter is mediated by quality and quantity of crop residues: mechanisms and thresholds. Biol Fert Soils 53:287–301

Shahbaz M, Kumar A, Kuzyakov Y, Borjesson G, Blagodatskaya E (2018) Priming effects induced by glucose and decaying plant residues on SOM decomposition: a three-source ^{13}C/^{14}C partitioning study. Soil Biol Biochem 121:138–146

Soares M, Rousk J (2019) Microbial growth and carbon use efficiency in soil: links to fungal-bacterial dominance, SOC-quality and stoichiometry. Soil Biol Biochem 131:195–205

Song XY, Spaccini R, Pan G, Piccolo A (2013) Stabilization by hydrophobic protection as a molecular mechanism for organic carbon sequestration in maize-amended rice paddy soils. Sci Total Environ 458:319–330

Spaccini R, Piccolo A, Conte P, Haberhauer G, Gerzabek MH (2002) Increased soil organic carbon sequestration through hydrophobic protection by humic substances. Soil Biol Biochem 34:1839–1851

Stenström J, Svensson K, Johansson M (2001) Reversible transition between active and dormant microbial states in soil. FEMS Microbiol Ecol 36:93–104

Straathof AL, Chincarini R, Comans RNJ, Hoffland E (2014) Dynamics of soil dissolved organic carbon pools reveal both hydrophobic and hydrophilic compounds sustain microbial respiration. Soil Biol Biochem 79:109–116

Sun Y, Huang S, Yu X, Zhang W (2015) Differences in fertilization impacts on organic carbon content and stability in a paddy and an upland soil in subtropical China. Plant Soil 397:189–200

Tian P, Mason-Jones K, Liu S, Wang Q, Sun T (2019) Form of nitrogen deposition affects soil organic matter priming by glucose and cellulose. Biol Fert Soils 55:383–391

von Lüetzow M, Kögel-Knabner I, Ekschmitt K, Matzner E, Guggenberger G, Marschner B, Flessa H (2006) Stabilization of organic matter in temperate soils: mechanisms and their relevance under different soil conditions—a review. Eur J Soil Sci 57:426–445

Wang J, Thornton B, Yao H (2014) Incorporation of urea-derived ^{13}C into microbial communities in four different agriculture soils. Biol Fert Soils 50:603–612

Wang D, Zhu Z, Shahbaz M, Chen L, Liu S, Inubushi K, Wu J, Ge T (2019) Split N and P addition decreases straw mineralization and the priming effect of a paddy soil: a 100-day incubation experiment. Biol Fert Soils 55:701–712

Wang YM, Li M, Jiang CY, Liu M, Wu M, Liu P, Li ZP, Uchimiya M, Yuan XY (2020) Soil microbiome-induced changes in the priming effects of ^{13}C-labelled substrates from rice residues. Sci Total Environ 726:138562

Xia Y, Chen X, Hu Y, Zheng S, Ning Z, Guggenberger G, He H, Wu J, Su Y (2019) Contrasting contribution of fungal and bacterial residues to organic carbon accumulation in paddy soils across eastern China. Biol Fert Soils 55:767–776

Xu Y, Chen Z, Fontaine S, Wang W, Luo J, Fan J, Ding W (2017) Dominant effects of organic carbon chemistry on decomposition dynamics of crop residues in a Mollisol. Soil Biol Biochem 115:221–232

Yuan H, Zhu Z, Liu S, Ge T, Jing H, Li B, Liu Q, Lynn TM, Wu J, Kuzyakov Y (2016) Microbial utilization of rice root exudates: ^{13}C labeling and PLFA composition. Biol Fert Soils 52:615–627

Zhou P, Pan GX, Spaccini R, Piccolo A (2010) Molecular changes in particulate organic matter (POM) in a typical Chinese paddy soil under different long-term fertilizer treatments. Eur J Soil Sci 61: 231–242